Progress In Electromagnetics Research C, Vol. 77, 57–68, 2017

Electromagnetic Spin Current Density of Surface Plasmon Polaritons

Shi Yao Chong and Jian-Qi Shen*

Abstract—A subject of *plasmonic spinphotonics* is developed for surface plasmon polaritons (SPPs). Since an electromagnetic field is a vectorial field, it has spinning angular momentum, and thus spin current is one of its degrees of freedom. A spin current density tensor has 24 independent components because of its antisymmetry in coordinate indices. By using the law of conservation of electromagnetic angular momentum (i.e., orbital angular momentum plus spinning angular momentum), the electromagnetic spin current density tensor is derived, and its characteristics are indicated. Since surface plasmon polaritons can exhibit various intriguing optical and electromagnetic effects and have many practical applications, we consider a new potential effect relevant to spin current transfer. The electromagnetic spin current density tensor and its intensity profile are analyzed for SPPs sustained on a metal-dielectric interface. The plasmonic spin on a metal ring and a straight thin metal belt is calculated, and based on this, a nanomechanical effect caused by *plasmonic spin current transfer* is suggested. It is expected that such a nontrivial nanomechanical effect will be useful in the design of new nanophotonic devices aiming at sensitive, accurate measurement techniques.

1. INTRODUCTION

Surface plasmon polaritons (SPPs) can be identified as electromagnetic eigenstates confined to an interface, of which the two adjacent media are usually an ordinary dielectric with positive permittivity and a metal with negative permittivity. Historically, the concept of SPPs originated from Ritchie's theoretical analysis of plasma losses relevant to fast electrons in 1957 [1]. In recent years, with current progress in a wealth of electromagnetic simulation methods and the state-of-the-art nano fabrication technologies, such as electron beam lithography [2], molecular beam epitaxy [3], and focussed ion beam [4], researches of various mechanisms and applications of SPPs have become increasingly intensive in a large number of fields [5, 6]. Surface plasmonics involves a variety of topics relevant to optics, photonics, electronics and many other interdisciplines, e.g., artificial metamaterials [7], surface-enhanced Raman scattering [8, 9], modern sensors [10], nanophotonic devices [11–13], and sub-wavelength optics [14].

Most of the degrees of freedom of SPPs, e.g., field intensity, energy density, polarization and phase, have been utilized in surface plasmonics. As far as we know, less attention has been paid to the spin current density of SPPs. In this paper, we will concentrate our attention on the electromagnetic spin current of SPPs as well as its potential applications in plasmonic nanomechanical effects. As well known, in spintronics (spin electronics), electron spin and its transfer dynamics have attracted considerable interest of many researchers [15,16]. For similar reasons, the duplicate of electron spin in photonics, i.e., plasmonic spin current, which will have important theoretical significance and potential applications in some areas of nanophotonic device design, should also deserve consideration. For example, the spin current density of SPPs may lead to some nontrivial mechanical effects, which can be utilized

Received 19 June 2017, Accepted 8 August 2017, Scheduled 21 August 2017
* Corresponding author: Jian-Qi Shen (jqshen@zju.edu.cn).
The authors are with the Centre for Optical and Electromagnetic Research, College of Optical Science and Engineering, State Key Laboratory of Modern Optical Instrumentations, East Building No. 5, Zijingang Campus, Zhejiang University, Hangzhou 310058, China.

in the design of new photonic devices such as nanoscale-sensitivity sensors and spin-transfer–based nanomechanical devices.

The present paper is organized as follows. First, we will address the concept of *electromagnetic spin current density tensor* by using the conservation law of electromagnetic angular momentum. Such a spin current density tensor has 24 independent components. We will obtain all the components for the SPPs on a metal-dielectric interface. The profiles of the nonzero components of the spin current density will be plotted for the SPPs. The volume integral of the SPPs spin current density will be evaluated, and based on this, a new nanomechanical effect, where the plasmonic spin transfer plays a key role, will be suggested for a thin metal film.

2. SPPS ON A METAL-DIELECTRIC SURFACE AND THE SPIN CURRENT DENSITY OF ELECTROMAGNETIC FIELD

Surface plasmon modes can be confined onto metal surfaces due to boundary conditions of the Maxwell fields. According to the dispersion relations, there can be two kinds of surface plasmon modes [15–17]: specifically, one is localized in metal nanoparticles, called "localized surface plasmons", which is not a propagating mode, and the other is bounded on the interface between a metal and a dielectric medium. Such surface modes can propagate through dozens of micrometers or even hundreds of micrometers along the surface, but decays exponentially into two neighboring media within a penetration depth of 200 or 300 nm perpendicular to the metal-dielectric interface [15–17]. Both of the surface plasmon modes can have spin current density and exhibit some nanomechanical effects caused by plasmonic spin current transfer. In this paper, we shall focus on only the propagating surface plasmon polaritons on the metal-dielectric interface, which is shown in Figure 1. Here medium 1 is an ordinary dielectric medium with positive relative dielectric constant, and medium 2 is a metal, of which the relative permittivity is $\varepsilon_2 = 1 - \omega_p^2/\omega^2$, where ω_p denotes the plasma frequency of metal. When the frequency of the electromagnetic wave $\omega < \omega_p$, the relative permittivity of medium 2 is negative. We assume that the plane of incidence for the SPPs eigenstate is zOx. The TM-mode SPPs can propagate in the z-direction, and its field decays exponentially in the x-direction.

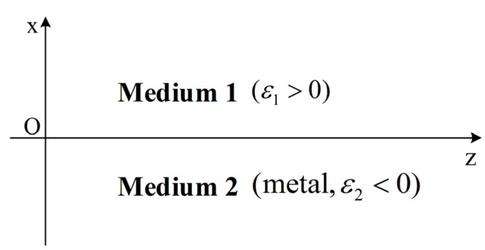

Figure 1. The geometric configuration of a metal-dielectric interface, which can support SPPs. The permittivity of one of the medium (say, medium 1) is positive, and the permittivity of the other medium (medium 2) is negative.

From the Maxwell equations and electromagnetic boundary conditions, the electric field strengths of the SPPs in both media are given by

$$\begin{cases} \mathbf{E}_1 = \mathbf{E}_1^{(0)} \exp\left(-\alpha_1 x\right) \exp\left[i\left(\beta z - \omega t\right)\right], & x > 0 \\ \mathbf{E}_2 = \mathbf{E}_2^{(0)} \exp\left(\alpha_2 x\right) \exp\left[i\left(\beta z - \omega t\right)\right], & x < 0 \end{cases} \tag{1}$$

where the attenuation coefficients are $\alpha_1 = \sqrt{\beta^2 - k_0^2\varepsilon_1}$ and $\alpha_2 = \sqrt{\beta^2 - k_0^2\varepsilon_2}$, and the phase constant is $\beta = k_0\sqrt{\frac{\varepsilon_1\varepsilon_2}{\varepsilon_1+\varepsilon_2}}$. Here, the vacuum wavenumber square is $k_0^2 = (\omega/c)^2$. Since α_1 and α_2 are positive, the electric field decays exponentially away from the interface of the two media. With the help of Gauss' law $\nabla \cdot \mathbf{E} = 0$ and Faraday's law of electromagnetic induction $\nabla \times \mathbf{E} = -\frac{\partial \mathbf{B}}{\partial t}$, the electric and magnetic field strengths in both media can be derived by using the electromagnetic boundary conditions [5, 6].

The result is given as follows

$$\begin{cases} \mathbf{E}_1 = \left(\frac{i\beta}{\alpha_1}E_{1z}^{(0)}, E_{1y}^{(0)}, E_{1z}^{(0)}\right)\exp\left(-\alpha_1 x\right)\exp\left[i\left(\beta z-\omega t\right)\right], \quad x>0 \\ \mathbf{E}_2 = \left(-\frac{i\beta}{\alpha_2}E_{2z}^{(0)}, E_{2y}^{(0)}, E_{2z}^{(0)}\right)\exp\left(\alpha_2 x\right)\exp\left[i\left(\beta z-\omega t\right)\right], \quad x<0 \end{cases} \tag{2}$$

$$\begin{cases} \mathbf{H}_1 = \frac{i}{\omega\mu_0}\left(i\beta E_{1y}^{(0)}, \frac{k_0^2\varepsilon_1}{\alpha_1}E_{1z}^{(0)}, \alpha_1 E_{1y}^{(0)}\right)\exp\left(-\alpha_1 x\right)\exp\left[i\left(\beta z-\omega t\right)\right], \qquad x>0 \\ \mathbf{H}_2 = \frac{i}{\omega\mu_0}\left(i\beta E_{2y}^{(0)}, -\frac{k_0^2\varepsilon_2}{\alpha_2}E_{2z}^{(0)}, -\alpha_2 E_{2y}^{(0)}\right)\exp\left(\alpha_2 x\right)\exp\left[i\left(\beta z-\omega t\right)\right]. \quad x<0 \end{cases} \tag{3}$$

Here $E_y^{(0)}$ and $E_z^{(0)}$ are the amplitudes of electric field in the y- and z-directions, respectively. In this situation, only the TM modes can exist, and according to the boundary conditions, we require $E_{1y}^{(0)} = E_{2y}^{(0)} = 0$.

Now we shall consider the spin current density tensor of electromagnetic field by using the conservation law of total angular momentum. From Noether's theorem [18], the canonical energy-momentum tensor, $T^{\mu\nu}$, of the electromagnetic field is given by

$$T^{\mu\nu} = -F^{\mu\sigma}\partial^\nu A_\sigma - \eta^{\mu\nu}\ell, \qquad \ell = -\frac{1}{4}F^{\mu\nu}F_{\mu\nu}, \tag{4}$$

where ℓ denotes the Lagrangian density of the electromagnetic field, and $F_{\mu\nu}$ is the electromagnetic field tensor, i.e., $F_{\mu\nu} = \partial_\mu A_\nu - \partial_\nu A_\mu$. Here, A_μ is a four-dimensional electromagnetic vector potential. The electric field and magnetic flux density can be written explicitly as $\frac{\mathbf{E}}{c} = -(F^{0x}, F^{0y}, F^{0z})$, $\mathbf{B} = -(F_{yz}, F_{zx}, F_{xy})$. $\eta^{\mu\nu} = \eta_{\mu\nu}$ is Minkowski metric with signature $(+,-,-,-)$, so that it has the metric components $\eta^{00} = 1, \eta^{11} = \eta^{22} = \eta^{33} = -1$, and the remainders are zero. Here, all the Greek letters represent the spacetime coordinate indices (0, x, y, z). The Einstein summation convention (i.e., sum over repeated indices) is implied in tensor calculation Eq. (4). Since $T^{\mu\nu}$ is neither a symmetric nor a gauge covariant energy-momentum tensor, its asymmetry in the indices μ, ν indicates that the electromagnetic field can exhibit a nonzero spin current density $s^{\mu\lambda\nu}$. The orbital angular momentum current density of the electromagnetic field can be defined as $L^{\mu\lambda\nu} = T^{\mu\nu}x^\lambda - T^{\mu\lambda}x^\nu$, where the indices μ, ν, λ range over 0, x, y, z [18]. By taking the four-dimensional covariant divergence of the *electromagnetic orbital angular momentum current density* and using the conservation law of electromagnetic energy and momentum (i.e., $\partial_\mu T^{\mu\nu} = 0$, $\partial_\mu T^{\mu\lambda} = 0$), one can obtain

$$\partial_\mu L^{\mu\lambda\nu} = T^{\mu\nu}\partial_\mu x^\lambda - T^{\mu\lambda}\partial_\mu x^\nu = T^{\lambda\nu} - T^{\nu\lambda}. \tag{5}$$

By using the relation in Eq. (4), the antisymmetric tensor $T^{\lambda\nu} - T^{\nu\lambda}$ yields

$$T^{\lambda\nu} - T^{\nu\lambda} = -F^{\lambda\sigma}\partial_\sigma A^\nu + F^{\nu\sigma}\partial_\sigma A^\lambda = -\partial_\sigma\left(F^{\lambda\sigma}A^\nu - F^{\nu\sigma}A^\lambda\right), \tag{6}$$

where the equation of motion of the free electromagnetic field (i.e., the Maxwell equation $\partial_\sigma F^{\lambda\sigma} = 0$, $\partial_\sigma F^{\nu\sigma} = 0$) is substituted. Now it follows from Eqs. (5) and (6) that a conservation law of the total angular momentum turns out to be in the form

$$\partial_\mu\left[L^{\mu\lambda\nu} + \left(F^{\lambda\mu}A^\nu - F^{\nu\mu}A^\lambda\right)\right] = 0. \tag{7}$$

Since $L^{\mu\lambda\nu}$ is an orbital angular momentum current density (tensor) of the electromagnetic field, from Eq. (7), the spinning angular momentum current density (tensor) of the electromagnetic field should be the form

$$s^{\mu\lambda\nu} = F^{\lambda\mu}A^\nu - F^{\nu\mu}A^\lambda. \tag{8}$$

The electromagnetic spin current density tensor $s^{\mu\lambda\nu}$ has the following properties: i) $s^{\mu\lambda\nu}$ is antisymmetric in its indices λ, ν, i.e., $s^{\mu\lambda\nu} = -s^{\mu\nu\lambda}$; ii) $s^{\mu\lambda\nu}$ has 24 independent components in a four-dimensional spacetime (since it is antisymmetric in indices λ, ν, there are 6 independent components

$\{\lambda\nu\}$, and the index μ corresponds to 4 independent components. Thus, there are 4×6 independent components in $s^{\mu\lambda\nu}$); iii) the electromagnetic spin current density (tensor) agrees with the relation $s^{\mu\lambda\nu} + s^{\nu\mu\lambda} + s^{\lambda\nu\mu} = 2(F^{\mu\nu}A^{\lambda} + F^{\lambda\mu}A^{\nu} + F^{\nu\lambda}A^{\mu})$.

We shall consider some of the components that have explicit physical meanings. When the superscript index $\mu = 0$, $s^{0\lambda\nu} = F^{\lambda 0}A^{\nu} - F^{\nu 0}A^{\lambda}$, which can be identified as the electromagnetic spin density, if λ and ν range over the spatial indices x, y, z. Since $F^{\lambda 0} = E^{\lambda}$ and $F^{\nu 0} = E^{\nu}$, the spin density vector $s^{0\lambda\nu}$ can be rearranged as

$$\mathbf{s} = \mathbf{E} \times \mathbf{A}, \tag{9}$$

where $\mathbf{A}$ is a three-dimensional magnetic vector potential. Note that expression (9) is a quantity in natural units [19]. In the international system of units (SI), the electromagnetic spin density turns out to be

$$\mathbf{s} = \varepsilon_0\varepsilon_r \cdot \mathrm{Re}(\mathbf{E}) \times \mathrm{Re}(\mathbf{A}), \tag{10}$$

where the electric field and magnetic vector potential are taken to be the real parts. When we derive the spin current density by using the concept of canonical energy-momentum tensor and the law of angular momentum conservation, i.e., Eq. (4) to Eq. (8), the electric field and magnetic vector potential are real vectors. However, in obtaining the explicit expressions for the electric field and magnetic vector potential of SPPs, i.e., Eq. (1) to Eq. (3), we use the complex field formalism. Therefore, in order to derive the instantaneous spin current density of SPPs, we should take the real parts of the electric field and magnetic vector potential of SPPs, as performed in Eq. (10).

In order to indicate the physical meaning of the spin density in Eqs. (9) and (10), as an illustrative example, we shall consider two polarization modes of a simple plane wave (i.e., left- and right-handed circularly polarized fields) in vacuum. The electric field vectors of the left- and right-handed polarized fields are given by

$$\begin{aligned} E_x^L &= E_0\cos(\omega t - kz), \quad E_y^L = E_0\sin(\omega t - kz), \\ E_x^R &= E_0\cos(\omega t - kz), \quad E_y^R = -E_0\sin(\omega t - kz), \end{aligned} \tag{11}$$

and the magnetic vector potentials, which can be defined as $\mathbf{E} = -\frac{\partial \mathbf{A}}{\partial t}$ under the condition of Coulomb gauge, are of the form

$$\begin{aligned} A_x^L &= -\frac{E_0}{\omega}\sin(\omega t - kz), \quad A_y^L = \frac{E_0}{\omega}\cos(\omega t - kz), \\ A_x^R &= -\frac{E_0}{\omega}\sin(\omega t - kz), \quad A_y^R = -\frac{E_0}{\omega}\cos(\omega t - kz), \end{aligned} \tag{12}$$

where the superscripts L, R represent the left- and right-handed circularly polarized fields, respectively. We shall calculate the electromagnetic spin vector $\mathbf{S} = \varepsilon_0 \int \mathbf{E} \times \mathbf{A} dV$ for both left- and right-handed circularly polarized fields. The nonzero spin density of the left-handed circularly polarized field is given by $s_z^L = \varepsilon_0(E_x^L A_y^L - E_y^L A_x^L) = \frac{\varepsilon_0 E_0^2}{\omega}$, and its volume integral is $S_z^L = \int s_z^L dV = \int \frac{\varepsilon_0 E_0^2}{\omega} dV$. It should be pointed out that for a quantized electromagnetic field (photon field), where the electric field E_0 is a second-quantized operator, the volume integral of the field energy density $\varepsilon_0 E_0^2$ is $\int \varepsilon_0 E_0^2 dV = \left(n^L + \frac{1}{2}\right)\hbar\omega$, where $\hbar$ denotes the reduced Planck constant; the integer n^L is a total number of photons; $\frac{1}{2}\hbar\omega$ stands for a quantum-vacuum zero-point fluctuation energy [18]. Therefore, the spin of the left-handed circular polarization is $S_z^L = \left(n^L + \frac{1}{2}\right)\hbar$, i.e., a left-handed circularly polarized photon has a spin with the magnitude of $\hbar$ and a vacuum mode has a spin of $\frac{1}{2}\hbar$. For the right-handed circularly polarized photon field, the spin density is given by $s_z^R = \varepsilon_0(E_x^R A_y^R - E_y^R A_x^R) = -\frac{\varepsilon_0 E_0^2}{\omega}$, and the volume integral is $S_z^R = \int s_z^R dV = -\int \frac{\varepsilon_0 E_0^2}{\omega} dV$. Then the spin of the right-handed circularly polarized quantized electromagnetic field is $S_z^R = -\left(n^R + \frac{1}{2}\right)\hbar$, where n^R is a total number of right-handed circularly polarized photons. Then the total spin is given by $S_z^{tot} = S_z^L + S_z^R = (n^L - n^R)\hbar$. If, for example, $n^L = n^R$ (i.e., for a linearly polarized mode), the total spin vanishes. Here, the spins of left- and right-handed polarized modes at quantum vacuum level are also exactly cancelled.

In the above, we have pointed out that $s^{0\lambda\nu}$ is a spin density, and the other components $s^{\mu\lambda\nu}$ are spin current densities, which are necessary in spin transfer dynamics in the future topics of *plasmonic spinphotonics*.

3. THE SPIN CURRENT DENSITY OF SURFACE PLASMON POLARITONS

In this section, we shall study all the nonzero components of the spin current density tensor of the SPPs. From Eq. (2) or Eq. (3), the magnetic vector potential of the surface plasmon polaritons on both sides of the interface can be obtained by using $\mathbf{B} = \nabla \times \mathbf{A}$ or $\mathbf{E} = -\frac{\partial \mathbf{A}}{\partial t}$:

$$\begin{cases} \mathbf{A}_1 = \dfrac{1}{i\omega}\left(\dfrac{i\beta}{\alpha_1}E_{1z}^{(0)}, E_{1y}^{(0)}, E_{1z}^{(0)}\right)\exp\left(-\alpha_1 x\right)\exp\left[i\left(\beta z - \omega t\right)\right], & x > 0 \\ \mathbf{A}_2 = \dfrac{1}{i\omega}\left(-\dfrac{i\beta}{\alpha_2}E_{2z}^{(0)}, E_{2y}^{(0)}, E_{2z}^{(0)}\right)\exp\left(\alpha_2 x\right)\exp\left[i\left(\beta z - \omega t\right)\right]. & x < 0 \end{cases} \tag{13}$$

Substituting Eq. (2) and Eq. (13) into Eq. (8), one can obtain the spin current density tensor of SPPs (in SI units). The tensor $s^{\mu\lambda\nu}$ has 64 (i.e., 4^3) components, and among them 24 are independent. It can be found that only seven of them are nonzero components for the present SPPs. We will list all these nonzero components: In medium 1, the spin current density can be expressed as

$$\begin{cases} s^{0zx} = \varepsilon_1\varepsilon_0\left(E_{1z}A_{1x} - E_{1x}A_{1z}\right) = \varepsilon_1\varepsilon_0\dfrac{\beta}{\omega\alpha_1}\left(E_{1z}^{(0)}\right)^2\exp\left(-2\alpha_1 x\right), \\ s^{xxz} = \varepsilon_1\varepsilon_0 B_{1y}A_{1x} = -\varepsilon_1\varepsilon_0\dfrac{\beta k_0^2\varepsilon_1}{\omega^2\alpha_1^2}\left(E_{1z}^{(0)}\right)^2\exp\left(-2\alpha_1 x\right)\sin(\beta z - \omega t)\cos(\beta z - \omega t), \\ s^{zzx} = -\varepsilon_1\varepsilon_0 B_{1y}A_{1z} = \varepsilon_1\varepsilon_0\dfrac{k_0^2\varepsilon_1}{\omega^2\alpha_1}\left(E_{1z}^{(0)}\right)^2\exp\left(-2\alpha_1 x\right)\sin^2(\beta z - \omega t), \\ s^{x0x} = -\varepsilon_1\varepsilon_0 E_{1x}A_{1x} = \varepsilon_1\varepsilon_0\dfrac{\beta^2}{\omega\alpha_1^2}\left(E_{1z}^{(0)}\right)^2\exp\left(-2\alpha_1 x\right)\sin(\beta z - \omega t)\cos(\beta z - \omega t), \\ s^{x0z} = -\varepsilon_1\varepsilon_0 E_{1x}A_{1z} = \varepsilon_1\varepsilon_0\dfrac{\beta}{\omega\alpha_1}\left(E_{1z}^{(0)}\right)^2\exp\left(-2\alpha_1 x\right)\sin^2(\beta z - \omega t), \\ s^{z0x} = -\varepsilon_1\varepsilon_0 E_{1z}A_{1x} = -\varepsilon_1\varepsilon_0\dfrac{\beta}{\omega\alpha_1}\left(E_{1z}^{(0)}\right)^2\exp\left(-2\alpha_1 x\right)\cos^2(\beta z - \omega t), \\ s^{z0z} = -\varepsilon_1\varepsilon_0 E_{1z}A_{1z} = -\varepsilon_1\varepsilon_0\dfrac{1}{\omega}\left(E_{1z}^{(0)}\right)^2\exp\left(-2\alpha_1 x\right)\sin(\beta z - \omega t)\cos(\beta z - \omega t), \end{cases} \tag{14}$$

and in medium 2, the spin current density can be written explicitly as

$$\begin{cases} s^{0zx} = \varepsilon_2\varepsilon_0\left(E_{2z}A_{2x} - E_{2x}A_{2z}\right) = -\varepsilon_2\varepsilon_0\dfrac{\beta}{\omega\alpha_2}\left(E_{1z}^{(0)}\right)^2\exp\left(2\alpha_2 x\right), \\ s^{xxz} = \varepsilon_2\varepsilon_0 B_{2y}A_{2x} = -\varepsilon_2\varepsilon_0\dfrac{\beta k_0^2\varepsilon_2}{\omega^2\alpha_2^2}\left(E_{1z}^{(0)}\right)^2\exp\left(2\alpha_2 x\right)\sin(\beta z - \omega t)\cos(\beta z - \omega t), \\ s^{zzx} = -\varepsilon_2\varepsilon_0 B_{2y}A_{2z} = -\varepsilon_2\varepsilon_0\dfrac{k_0^2\varepsilon_2}{\omega^2\alpha_2}\left(E_{1z}^{(0)}\right)^2\exp\left(2\alpha_2 x\right)\sin^2(\beta z - \omega t), \\ s^{x0x} = -\varepsilon_2\varepsilon_0 E_{2x}A_{2x} = \varepsilon_2\varepsilon_0\dfrac{\beta^2}{\omega\alpha_2^2}\left(E_{1z}^{(0)}\right)^2\exp\left(2\alpha_2 x\right)\sin(\beta z - \omega t)\cos(\beta z - \omega t), \\ s^{x0z} = -\varepsilon_2\varepsilon_0 E_{2x}A_{2z} = -\varepsilon_2\varepsilon_0\dfrac{\beta}{\omega\alpha_2}\left(E_{1z}^{(0)}\right)^2\exp\left(2\alpha_2 x\right)\sin^2(\beta z - \omega t), \\ s^{z0x} = -\varepsilon_2\varepsilon_0 E_{2z}A_{2x} = \varepsilon_2\varepsilon_0\dfrac{\beta}{\omega\alpha_2}\left(E_{1z}^{(0)}\right)^2\exp\left(2\alpha_2 x\right)\cos^2(\beta z - \omega t), \\ s^{z0z} = -\varepsilon_2\varepsilon_0 E_{2z}A_{2z} = -\varepsilon_2\varepsilon_0\dfrac{1}{\omega}\left(E_{1z}^{(0)}\right)^2\exp\left(2\alpha_2 x\right)\sin(\beta z - \omega t)\cos(\beta z - \omega t). \end{cases} \tag{15}$$

Here, s^{0zx} is the nonzero component of the spin density $\mathbf{s}$ that has been mentioned in Eqs. (9) and (10). Its volume integral $\mathbf{S} = \int \varepsilon_0\varepsilon_r \cdot \mathrm{Re}(\mathbf{E}) \times \mathrm{Re}(\mathbf{A})dV$ is the spin vector (spinning angular momentum) of the SPPs. By using the second quantization procedure for $\mathbf{S}$ [18], such a spinning angular momentum operator of a quantized electromagnetic field, which has discrete eigenvalues, can be obtained. Now as a tentative study, we shall be primarily concerned with the first-quantization characteristics of the spin current, i.e., the intensity profile of all the nonzero components of the spin current density of SPPs. The distribution of the spin density component s^{0zx} is shown in Figure 2, where the magnitude of s^{0zx} has been normalized, and the unit of the space coordinates is c/ω_0 with ω_0 the angular frequency of the SPPs. In subgraph (a) of Figure 2 there is a cross-sectional diagram of s^{0zx} component in medium 1, and in subgraph (b) there is its distribution on both sides of the interface. In both media of the interface, the magnitude of s^{0zx} decays exponentially in the x-direction. While in the z-direction, it is uniform (i.e., independent of the coordinate z). The distributions of the other 6 nonzero components of the spin current density in the x-z plane are plotted in Figures 3–5. It can be found that all these spin current density components (s^{xxz}, s^{zzx}, s^{x0x}, s^{z0x}, s^{x0z} and s^{z0z}) oscillate in the z-direction, and they diminish exponentially in the x-direction. In Figures 2–5 for the plasmonic spin current density distribution, the parameter ωt in Eq. (15) is zero, and the phase constant β and attenuation coefficients α_1, α_2 of the SPPs are chosen as $\sqrt{6}\omega_0/c$ and $\sqrt{3}\omega_0/c$, $3\omega_0/c$, respectively.

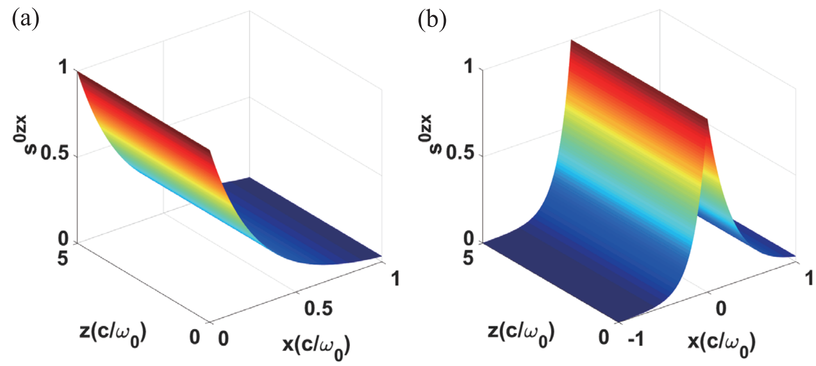

Figure 2. The spatial distribution of the spin current density component s^{0zx}. The profiles of s^{0zx} in medium 1 ($x > 0$) and in both medium 1 ($x > 0$) and medium 2 ($x < 0$) are plotted in subgraph (a) and subgraph (b), respectively. This spin current density component s^{0zx} is uniform in the z-direction and it decays exponentially in the x-direction.

In the present paper, we will suggest the plasmonic nanomechanical effect of SPPs based on the analysis of **S**. All the other nonzero components given in Eqs. (14) and (15) can in principle be used to investigate the plasmonic spin current transfer in nanomechanical device design.

4. THE SPINNING ANGULAR MOMENTUM AND MECHANICAL EFFECT OF SPPS

In order to suggest a plasmonic nanomechanical effect caused by SPPs spin transfer, first we shall evaluate the nonzero y-component of the vector of SPPs

$$S^y = S^{0zx} = \int_{-\infty}^{+\infty} s^{0zx} dxdydz. \tag{16}$$

Since s^{0zx} is independent of the spatial coordinates y and z, we can assume $\int dydz = \mathcal{A}$ with $\mathcal{A}$ an area on the y-z plane. By substituting the explicit expression s^{0zx} given in Eqs. (14) and (15) into Eq. (16), S^y has the form

$$\begin{aligned} S^y &= \varepsilon_0 \left(E_{1z}^{(0)}\right)^2 A \left(\int_{-\infty}^{0} \varepsilon_1 \frac{\beta}{\omega\alpha_1} \exp\left(-2\alpha_1 x\right) dx + \int_{0}^{+\infty} -\varepsilon_2 \frac{\beta}{\omega\alpha_2} \exp\left(2\alpha_2 x\right) dx\right) \\ &= \varepsilon_0 \left(E_{1z}^{(0)}\right)^2 A \left(\varepsilon_1 \frac{\beta}{\omega\alpha_1}\frac{1}{2\alpha_1} - \varepsilon_2 \frac{\beta}{\omega\alpha_2}\frac{1}{2\alpha_2}\right). \end{aligned} \tag{17}$$

By using the relation $\frac{\varepsilon_1}{\alpha_1} = -\frac{\varepsilon_2}{\alpha_2}$ for the SPPs, the y-component S^y of the plasmonic spin can be rearranged as

$$S^y = \varepsilon_0 \left(E_{1z}^{(0)}\right)^2 \mathcal{A} \frac{\varepsilon_1 \beta}{\omega\alpha_1} \left(\frac{1}{\alpha_1} + \frac{1}{\alpha_2}\right). \tag{18}$$

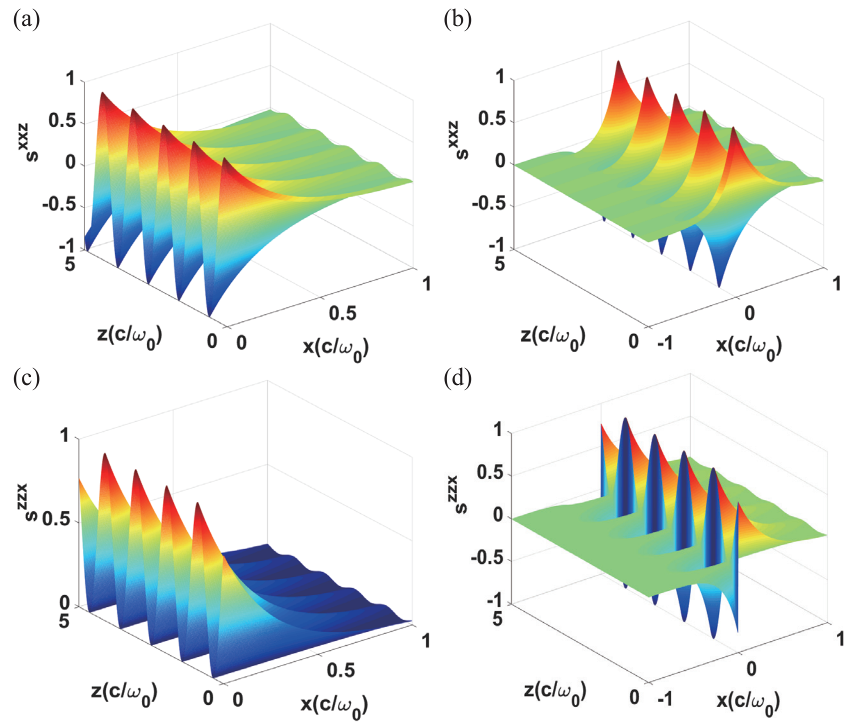

Figure 3. The spatial distribution of the spin current density components s^{xxz} and s^{zzx}. The distribution of s^{xxz} in medium 1 ($x > 0$) and in both medium 1 ($x > 0$) and medium 2 ($x < 0$) is plotted in subgraph (a) and subgraph (b), respectively; The distribution of s^{zzx} in medium 1 ($x > 0$) and in both medium 1 ($x > 0$) and medium 2 ($x < 0$) is plotted in subgraph (c) and subgraph (d), respectively. These two spin current density components (s^{xxz} and s^{zzx}) are oscillating in the z-direction and they diminish exponentially in the x-direction.

If medium 1 is vacuum or air and medium 2 a metal, then the attenuation coefficients α_1 and α_2 are given by

$$\begin{cases} \alpha_1 = \sqrt{-\dfrac{\varepsilon_1^2}{\varepsilon_1+\varepsilon_2}}\dfrac{\omega}{c} = \sqrt{-\dfrac{1}{1+\varepsilon_2}}\dfrac{\omega}{c}, \\ \alpha_2 = \sqrt{-\dfrac{\varepsilon_2^2}{\varepsilon_1+\varepsilon_2}}\dfrac{\omega}{c} = \sqrt{-\dfrac{\varepsilon_2^2}{1+\varepsilon_2}}\dfrac{\omega}{c}. \end{cases} \tag{19}$$

Then we have

$$\frac{1}{\alpha_1} + \frac{1}{\alpha_2} = \sqrt{-(1+\varepsilon_2)}\frac{c}{\omega}\left(1 - \frac{1}{\varepsilon_2}\right). \tag{20}$$

By substituting the result in Eq. (20) into S^y given in Eq. (18), we can obtain

$$S^y = \frac{1}{2}\varepsilon_0 \left(E_{1z}^{(0)}\right)^2 \mathcal{A}\frac{c}{\omega^2}\sqrt{\varepsilon_2(1+\varepsilon_2)}\left(1 - \frac{1}{\varepsilon_2}\right). \tag{21}$$

This is the plasmonic spin in the y-direction (also in the direction of the magnetic field **H** of the TM-mode SPPs).

Now we shall suggest our scenario of nanomechanical effect via plasmonic spin current transfer between surface plasmon modes and a thin metallic film belt. We assume that a metal ring (formed by the thin metallic film) is suspended in air, which is shown in Figure 6. Here, the suspension wire is along the Y axis. We assume that the surface plasmon modes have been excited on the metal ring. One can use Otto or Kretchmann prism to excite SPPs on the metallic ring, but some special customized clamping mechanisms and optical systems are surely required. Besides Otto or Kretchmann technique,

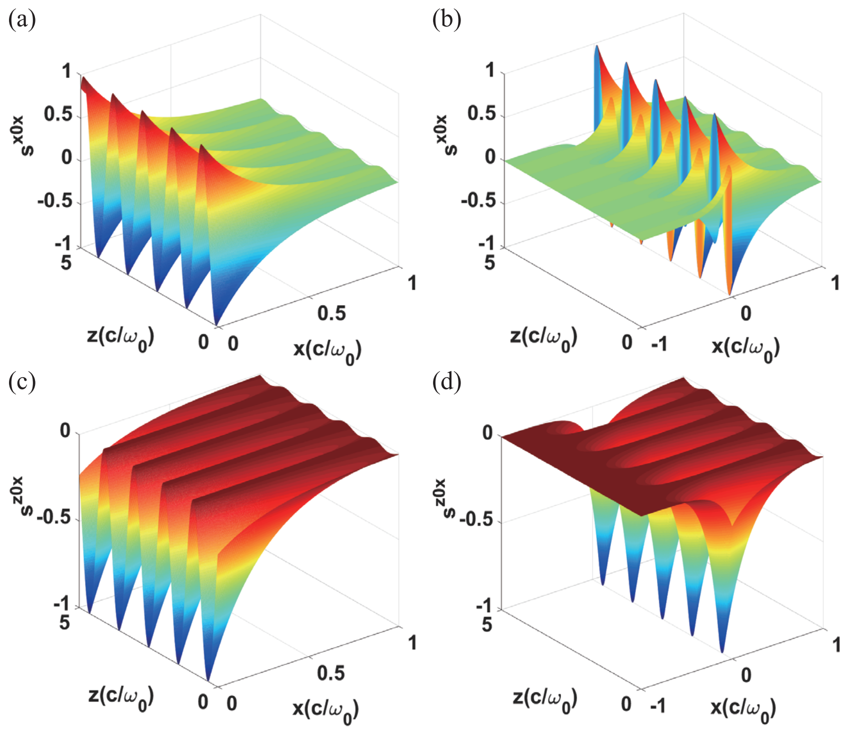

Figure 4. The spatial distribution of the spin current density components s^{x0x} and s^{z0x}. The distribution of s^{x0x} in medium 1 ($x > 0$) and in both medium 1 ($x > 0$) and medium 2 ($x < 0$) is plotted in subgraph (a) and subgraph (b), respectively; The distribution of s^{z0x} in medium 1 ($x > 0$) and in both medium 1 ($x > 0$) and medium 2 ($x < 0$) is plotted in subgraph (c) and subgraph (d), respectively. These two spin current density components (s^{x0x} and s^{z0x}) are oscillating in the z-direction and they diminish exponentially in the x-direction.

one can also fabricate a grating structure on the metallic ring surface. Such a grating structure can provide extra momentum in the direction of propagation, so that SPPs can be excited. The grating structure only occupies a small part of the metallic ring, so it does not dramatically affect the standing wave state of SPPs. In the present scenario, we choose the relative dielectric constant of the metal $\varepsilon_2 = -10$, the wavelength of incident light (for exciting the SPPs) $\lambda = 200\pi$ nm, and then the angular frequency of the light $\omega = \frac{2\pi c}{\lambda} = 3 \times 10^{15}$ rad $\cdot$ s^{-1}. We shall evaluate the field strength of the excited SPPs on the metal ring. It should be noted that the brightness of current state-of-the-art fiber-coupled broad-area diodes can be in the range of $1.8 \sim 6.0\,\mathrm{MW/cm^2}$ [20]. If, for example, we choose a power density of $6.0\,\mathrm{MW/cm^2}$, the electric field of the applied laser field corresponds to $4.8 \times 10^6\,\mathrm{V/m}$. In general, because of the effect of strong confinement, the field strength of the SPPs excited by such a laser field can be a few times as strong as the laser field. Then we can assume that the SPPs field strength $E_{1z}^{(0)}$ has the order of magnitude of $1.0 \times 10^7\,\mathrm{V/m}$. The length, width and thickness of the metal ring can be chosen as $10\lambda_z$, 0.5 µm and 50 nm, respectively, with $\lambda_z = \frac{2\pi}{\beta}$. Under this condition, the penetration depth of SPPs into the metal is $30\,nm$, so SPPs only exist on one of the interfaces. Now by substituting these parameters into Eq. (21), we can obtain the spinning angular momentum $S^y = 4.6 \times 10^{-32}\,\mathrm{kg \cdot m^2/s}$ for the SPPs sustained on the metal ring.

It should be pointed out that the Ohmic loss of the metal can give rise to Joule heat. Such a strong SPPs field ($E_{1z}^{(0)} \simeq 1.0 \times 10^7\,\mathrm{V/m}$) will fuse or burn the metal ring at a thin spot, and the ring will immediately become a straight metal belt, as shown in Figure 7. Now the SPPs, which are supported on the straight metal belt, will change its original standing state (on the ring) to a new state (on the planar interface). If the following momentum-match condition holds

$$k_0 < \beta = k_0 \sqrt{\frac{\varepsilon_1 \varepsilon_2}{\varepsilon_1 + \varepsilon_2}} < k_0 n_{back}, \tag{22}$$

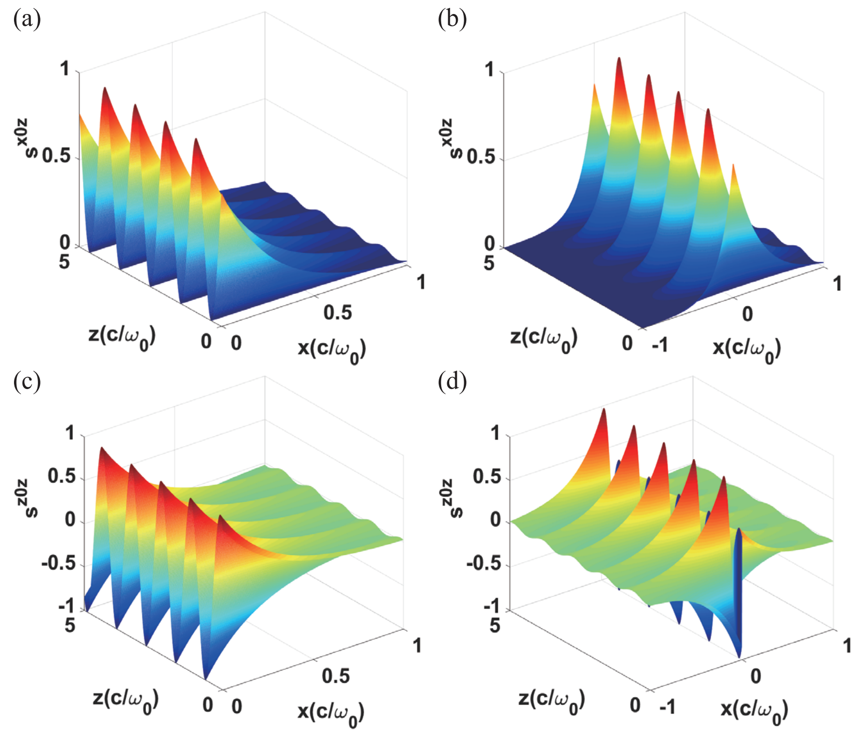

Figure 5. The spatial distribution of the spin current density components s^{x0z} and s^{z0z}. These two spin current density components (s^{x0z} and s^{z0z}) are oscillating in the z-direction and they diminish exponentially in the x-direction. The density of s^{x0z} in medium 1 ($x > 0$) is shown in subgraph (a) and its density in both medium 1 ($x > 0$) and medium 2 ($x < 0$) is in subgraph (b); The distribution of s^{z0z} in medium 1 ($x > 0$) is plotted in subgraph (c) and its density in both medium 1 ($x > 0$) and medium 2 ($x < 0$) is in subgraph (d).

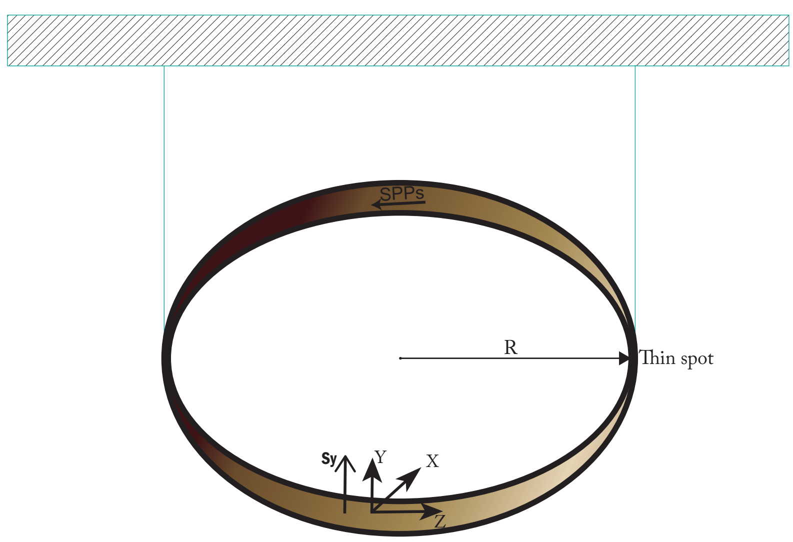

Figure 6. A metal ring, on which SPPs can be sustained. Such surface plasmon modes form standing wave, which satisfies a relation: $2\pi R = m\lambda_z$ with $\lambda_z = \frac{2\pi}{\beta}$. Here, m is an integer. The SPPs mode has a nonzero spin S^y, which is perpendicular to the circular torus.

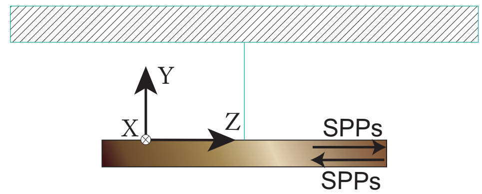

Figure 7. A straight thin metal belt, on which the SPPs can be sustained. Since the Ohmic loss of metal can give rise to the Joule heat, a strong SPPs field (e.g., $E_{1z}^{(0)} \simeq 1.0 \times 10^7\,\mathrm{V/m}$) would fuse or burn the metal ring (Figure 6) at a thin spot, and the ring will immediately become a straight metal belt. Since the SPPs mode will form a new standing wave on the present straight metal surface, it has a zero spin S^y, namely, the nonzero spin S^y of the SPPs on the metal ring has been transferred to the straight metal belt itself.

where n_{back} is the refractive index of surrounding medium, SPPs can radiate out. But under our condition, the surrounding of metal ring is vacuum or air, i.e., Eq. (22) is unsatisfied, and hence SPPs will be reflected backwards at the ends of the straight metal belt. As a result, SPPs will be reflected between two ends of the metal belt, and finally it will evolve into a new stationary state, which is a standing wave mode. Note that on the metal ring (in Figure 6), the standing-wave SPPs modes and ring scale should obey the following relation: the ring circumference $2\pi R$ is integer multiple of the wavelength of the SPPs, i.e., $2\pi R = m\lambda_z$. So when $m = 10$, both $2\pi R = m\lambda_z$ and $\lambda_z = 2\pi/\beta$ will be satisfied: specifically, from these two relations, we can obtain $2\pi R = m \cdot 2\pi/\beta$, i.e., $R = m/\beta$. If a metal ring with a radius fulfilling $R = m/\beta$ could be fabricated, the excited SPPs standing wave modes would possibly form on the metal ring. On the straight metal belt (in Figure 7), however, the metal belt length is integer multiple of the half wavelength of the SPPs, i.e., $l_z = n\frac{\lambda_z}{2}$. Here, $l_z = 2\pi R$. Thus, the mode indices n and m on the straight metal belt and the metal ring, respectively, agree with the relation $n = 2m$. Clearly, the spin density s'^{0zx} of such a new standing SPPs wave on the planar interface vanishes. This, therefore, means that the spinning angular momentum $S^y = 4.6 \times 10^{-32}\,\mathrm{kg \cdot m^2/s}$ of the original SPPs on the metal ring has been transferred to the thin metal belt, and such a thin metal belt can rotate because of its angular momentum $L = S^y$ acquired from the SPPs. Suppose that the density of metal is $\rho = 8.0 \times 10^3\,\mathrm{kg/m^3}$, and then the mass of metal is $1.2 \times 10^{-16}\,\mathrm{kg}$. The moment of inertia (rotational inertia) about the suspension wire (axis of rotation) is $J = \frac{1}{12}ml^2 = 3.9 \times 10^{-30}\,\mathrm{kg \cdot m^2}$, where l denotes the length of the straight metal belt. By using the definition of angular momentum $L = J\Omega$, one can arrive at the angular velocity of the metal belt $\Omega = 1.2 \times 10^{-2}\,\mathrm{rad/s}$. Due to change of geometric configuration of metal belt, such a rotational frequency of the metal belt is caused by the plasmonic spin current transfer from the SPPs to the straight metal belt.

In the literature, there have been some designs of nanomechanical photonic devices [21–25] by taking advantage of transfer of energy, momentum or angular momentum from electromagnetic fields (at both classical and quantum levels) to electromagnetic media, including time crystals [23,24], quantum wheels and "perpetuum mobile" of the third and fourth kinds [25]. All such new possible devices will exhibit motion (e.g., rotation, precession and nutation) of the electromagnetic materials. In this paper, we have suggested an alternative nanomechanical effect, which can be utilized to design sensitive, accurate techniques of measurement (e.g., nanoscale-sensitivity sensors).

5. CONCLUDING REMARKS

In this paper, we have considered the distribution profile of electromagnetic spin current density tensor of SPPs bound to a metal-dielectric interface. The spin current density of an electromagnetic field can be derived from the conservation law of total angular momentum (electromagnetic orbital angular momentum plus spinning angular momentum). The electromagnetic spin current density tensor has 24 independent components. As far as the SPPs sustained on a metal-dielectric interface is concerned, there are only 7 nonzero ones in the spin current density tensor. Since SPPs on the metal ring carry a spinning angular momentum, it can be expected that the nonzero spin density of such SPPs will exhibit some novel mechanical effects, namely, an effect of spin current transfer at nanomechanical level is suggested in this paper. Before the metal ring has been fused due to Joule heat production, SPPs, which are sustained on the metal ring, form a standing wave, which has nonzero spin. If, however, the metal ring becomes a straight belt, the new standing wave mode of SPPs has no spin, i.e., the lost angular momentum of SPPs has been transmitted to the thin metal belt and will cause its rotation around the suspension wire. The plasmonic spin density has been taken into account in order to evaluate the relevant observational physical quantities such as angular momentum and rotational angular frequency acquired by the nanoscale thin metal belt during this process of plasmonic spin transfer. The spatial distribution of the other nonzero spin current density components of SPPs, which can be used to study the problems of spinphotonic dynamics (such as how the spin density of SPPs is transferred to the nanoscale metal belt and how long it takes SPPs to transfer its spin to the metal belt), have also been demonstrated in this paper. Such a nanomechanical effect resulting from plasmonic spinning angular momentum transfer will find potential applications in the design of new nano-photonic devices such as accurate sensors (nanoscale-sensitivity rotational motion sensor).

ACKNOWLEDGMENT

This work is supported in part by the Natural Science Foundations of Zhejiang Province (China) under Project No. LY16A040002 as well as by the National Natural Science Foundations of China under Grants Nos. 61605170 and 11174250. Shen is also grateful to the Foundations of "Program of Zhejiang Leading Team of Science and Technology Innovation".

REFERENCES

1. Ritchie, R. H., "Plasma losses by fast electrons in thin films," *Phys. Rev.*, Vol. 1, No. 5, 874–881, 1957.
2. Vieu, C., F. Carcenac, A. Pepin, Y. Chen, M. Mejias, A. Lebib, L. Manin-Ferlazzo, L. Couraud, and H. Launois, "Electron beam lithography: resolution limits and applications," *Appl. Surf. Sci.*, Vol. 164, No. 4, 111–117, 2000.
3. Chen, Y., D. M. Bagnall, H. Koh, et al., "Plasma assisted molecular beam epitaxy of ZnO on c-plane sapphire: growth and characterization," *J. Appl. Phys.*, Vol. 84, No. 7, 3912–3918, 1998.
4. Giannuzzi, L. A. and F. A. Stevie, *Introduction to Focused Ion Beams: Instrumentation, Theory, Techniques and Practice*, Springer, Berlin, 2005.
5. Zayats, A. V., I. I. Smolyaninov, and A. A. Maradudin, "Nano-optics of surface plasmon polaritons," *Phys. Rep.*, Vol. 408, No. 3, 131–314, 2005.
6. Pitarke, J. M., V. M. Silkin, E. V. Chulkov, and P. M. Echenique, "Theory of surface plasmons and surface-plasmon polaritons," *Rep. Prog. Phys.*, Vol. 70, No. 1, 1–87, 2007.
7. Fang, N., H. Lee, C. Sun, and X. Zhang, "Sub-diffraction-limited optical imaging with a silver superlens," *Science*, Vol. 308, No. 5721, 534–537, 2005.
8. Fleischmann, M., P. J. Hendra, and A. J. Mcquillan, "Raman spectra of pyridine adsorbed at a silver electrode," *Chem. Phys. Lett.*, Vol. 26, No. 2, 163–166, 1974.
9. Jeanmaire, D. L., and R. P. V. Duyne, "Surface raman spectroelectrochemistry: Part I. Heterocyclic, aromatic, and aliphatic amines adsorbed on the anodized silver electrode," *J. Electroanal. Chem. Interfac.*, Vol. 84, No. 1, 1–20, 1977.
10. Homola, J., S. S. Yee, and G. Gauglitz, "Surface plasmon resonance sensors: review," *Sens. Actuators, B*, Vol. 54, No. 2, 3–15, 1999.
11. Frey, H. G., S. Witt, K. Felderer, and R. Guckenberger, "High-resolution imaging of single fluorescent molecules with the optical near-field of a metal tip," *Phys. Rev. Lett.*, Vol. 93, No. 20, 200801, 2004.
12. Tang, L., S. E. Kocabas, S. Latif, A. K. Okyay, D. S. Lygagnon, K. C. Saraswat, and D. A. B. Miller, "Nanometre-scale germanium photodetector enhanced by a near-infrared dipole antenna," *Nature Photon.*, Vol. 2, No. 4, 226–229, 2008.

13. Bozhevolnyi, S. I., V. S. Volkov, E. Devaux, J. Y. Laluet, and T. W. Ebbesen, "Channel plasmon subwavelength waveguide components including interferometers and ring resonators," *Nature*, Vol. 440, No. 7083, 508, 2006.
14. Gu, B. Y., "Surface plasmon subwavelength optics: principles and novel effects," *Physics (WuLi, Beijing)*, Vol. 36, No. 4, 280–287, 2007.
15. Maekawa, S., H. Adachi, K. Uchida, J. I. Ieda, and E. Saitoh, "Spin current: experimental and theoretical aspects," *J. Phys. Soc. Jpn.*, Vol. 82, No. 10, 102002, 2013.
16. Shen, S. Q., "Spintronics and spin current," *Physics (WuLi, Beijing)*, Vol. 37, No. 1, 16–23, 2008.
17. Maier, S. A., *Plasmonics: Fundamentals and Applications*, Chapt. 2 and 5, Springer, Berlin, 2007.
18. Bjorken, J. D. and S. D. Drell, *Relativistic Quantum Fields*, Chapt. 14, Mcgraw-Hill Companies, Inc., New York, 1965.
19. Guidry, M., *Gauge Field Theories: An Introduction with Applications*, Wiley, New York, 1992.
20. Injeyan, H. and G. D. Goodno, *High-Power Laser Handbook*, Chapt. 15, 445, McGraw-Hill Companies, Inc., New York, 2011.
21. Shen, J. Q., M. Norgren, and S. He, "Negative refraction and quantum vacuum effects in gyroelectric chiral medium and anisotropic magnetoelectric material," *Ann. Phys.*, Vol. 15, No. 12, 894–910, 2006.
22. Shen, J. Q., "Momentum transfer between quantum vacuum and anisotropic medium," *Prog. Theor. Phys. (Japan)*, Vol. 119, No. 3, 351–360, 2008.
23. Shapere, A. and F. Wilczek, "Classical time crystals," *Phys. Rev. Lett.*, Vol. 109, No. 16, 160402, 2012.
24. Zhao, L., "Strange Lagrangian systems and statistical mechanics," *J. Phys. A*, Vol. 46, No. 46, 493–494, 2013.
25. Chernodub, M. N., "Permanently rotating devices: extracting rotation from quantum vacuum fluctuations," arXiv: 1203.6588 [quant-ph].